Tunable Energy Transfer from Dicyanoaurate(I) and Dicyanoargentate(I) Donor Ions to Terbium(III) Acceptor Ions in Pure Crystals

Manal A. Rawashdeh-Omary,[†,‡] C. L. Larochelle,[§] and Howard H. Patterson*[,†]

Department of Chemistry and Department of Physics and Astronomy, University of Maine, Orono, Maine 04469

Received May 10, 1999

A temperature-dependent photoluminescence study is reported for single crystals of $M[Au(CN)_2]_3$ and $M[Ag(CN)_2]_3$ (M = Tb; Gd; Y). The results indicate that in both $Tb[Au(CN)_2]_3$ and $Tb[Ag(CN)_2]_3$ exclusive excitation of the donor leads to sensitized luminescence for the acceptor, characteristic of the $^5D_4 \rightarrow {}^7F_J$ ($J = 0-6$) transition of Tb(III). However, the sensitized luminescence is much stronger in $Tb[Ag(CN)_2]_3$ than in $Tb[Au(CN)_2]_3$ due to a larger spectral overlap between the $[Ag(CN)_2^-]$ emission and the Tb(III) absorption. Upon increasing the temperature, energy transfer is enhanced in $Tb[Ag(CN)_2]_3$ but inhibited in $Tb[Au(CN)_2]_3$. In $Tb[Ag(CN)_2]_3$, a large spectral overlap exists between the $[Ag(CN)_2^-]$ donor emission and the Tb(III) acceptor absorption at all temperatures. The Tb(III) sensitized emission is strong at all temperatures and is enhanced upon a temperature increase while the $[Ag(CN)_2^-]$ emission is quenched. An activation energy of 53.7 cm^{-1} (± 2.5 cm^{-1}) has been calculated for the energy transfer process in $Tb[Ag(CN)_2]_3$. In $Tb[Au(CN)_2]_3$, the Tb(III) sensitized luminescence decreases upon increasing the temperature. The $[Au(CN)_2^-]$ emission is strong and does not undergo a complete quenching as the temperature increases toward room temperature. The $[Au(CN)_2^-]$ emission undergoes a red shift upon cooling, which leads to an increased spectral overlap with the $^5D_4 \rightarrow {}^7F_6$ absorption band of Tb(III); thus energy transfer is *tuned* by controlling the temperature. The sensitized luminescence intensity of Tb(III) in $Tb[Au(CN)_2]_3$ is directly proportional to the numerical value of the donor−acceptor spectral overlap, in agreement with the theory of radiationless energy transfer.

Introduction

The area of energy transfer involving lanthanide ions has intrigued chemists, physicists, materials scientists, and biochemists due to the large number of applications in their respective disciplines.[1−4] Lanthanide ions have been used to "probe" many structural and analytical problems such as the determination of local symmetries in crystalline inorganic materials,[5a] catalysis,[5b] probing the structure of biological macromolecules,[6] and immunoassay using time-resolved luminescence.[7] In inorganic systems, lanthanide ions have been used with pure or doped solids of oxides[5a,8] and inorganic salts[9] in order to understand the molecular and electronic structures of these systems, or to assess their potential use as solid-state photonic devices.[10] The search for new solid-state materials containing lanthanide ions is the goal of many advancements in the laser and telecommunication technologies.[11]

Of special importance has been the study of lanthanide ion complexes of low-dimensional layered inorganic solids, due to the interesting structural and optical properties of these systems. Examples include the sensitized luminescence from lanthanide ions in complexes of uranyl phosphates and tetracyanoplatinates(II).[12] Our group has been studying the structure and spectroscopy of dicyano coordination compounds of Ag(I) and Au(I).[13−19] These compounds exhibit an unusual structure that consists of $[Ag(CN)_2^-]$ or $[Au(CN)_2^-]$ layers alternating with layers of the

[†] Department of Chemistry.
[‡] Present address: Department of Chemistry, Texas A&M University, College Station, TX 77843.
[§] Department of Physics and Astronomy.

(1) Powell, R. C.; Blasse, G. *Struct. Bonding* **1980**, *42*, 43.
(2) Wolf, H. C. *Adv. At. Mol. Phys.* **1967**, *3*, 119.
(3) Powell, R. C.; Soos, Z. G. *J. Lumin.* **1975**, *11*, 1.
(4) (a) Lakowicz, J. R. *Principles of Fluorescence Spectroscopy*; Plenum Press: New York, 1983; Chapter 10. (b) Dale, R. E.; Eisinger, J. In *Biochemical Fluorescence Concepts*; Chen, R. F., Edelhoch, H., Eds.; Marcel Dekker: New York, 1975; pp 115−284.
(5) (a) Morrison, C. A.; Leavitt, R. P. In *Handbook on the Physics and Chemistry of Rare Earths*; Gschneidner, K. A., Jr., Eyring, L., Eds.; North-Holland: Amsterdam, 1982; Vol. 9, Chapter 46. (b) Tanguay, J. F.; Suib, S. L. *Catal. Rev. Sci. Eng.* **1987**, *29*, 1.
(6) (a) Horrocks, W. DeW., Jr.; Sudnick, D. R. *Acc. Chem. Res.* **1981**, *14*, 384. (b) Horrocks, W. DeW., Jr. *Adv. Inorg. Biochem.* **1982**, *4*, 201. (c) Meares, C. F.; Wensel, T. G. *Acc. Chem. Res.* **1984**, *17*, 202. (d) Bünzli, J. C. G. *Inorg. Chim. Acta* **1987**, *139*, 219. (e) Bruno, J.; Horrocks, W. DeW., Jr.; Beckingham, K. *Biophys. Chem.* **1996**, *63*, 1. (f) Maune, J. F.; Klee, C. B.; Beckingham, K. *J. Biol. Chem.* **1992**, *267*, 5286.
(7) (a) Soini, E.; Lovgren, T. *CRC Crit. Rev. Anal. Chem.* **1987**, *18*, 105. (b) Hemmnilä, I. *Scand. J. Clin. Lab. Invest.* **1988**, *48*, 389.
(8) Dexpert-Ghys, J.; Faucher, M.; Caro, P. *Phys. Rev. B* **1981**, *23*, 607.
(9) (a) Blasse, G.; Dirksen, G. J.; van Vliet, J. P. M. *Inorg. Chim. Acta* **1988**, *142*, 165. (b) Hölsa, J.; Porcher, J. *Chem. Phys.* **1982**, *76*, 2790. (c) Jørgesen, C. K.; Reisfeld, R. *Struct. Bonding* **1982**, *100*, 127.
(10) (a) Auzel, F. *Proc. IEEE* **1973**, *61*, 758 and references cited therein. (b) Hehlen, M. P.; Krämer, K.; Güdel, H. U.; McFarlane, R. M.; Schwartz, R. N. *Phys. Rev. B* **1994**, *49*, 12475. (c) Hehlen, M. P.; Krämer, K.; Güdel, H. U. *J. Lumin.* **1994**, *60/61*, 142. (d) Riedener, T.; Krämer, K.; Güdel, H. U. *Inorg. Chem.* **1995**, *34*, 2745.
(11) (a) *Handbook of the Physics and Chemistry of the Rare Earths*; Gschneider, K. A., Eyring, L., Eds.; North-Holland: New York, 1979; Vols. 3 and 4. (b) *The Rare Earths in Modern Science and Technology*; McCarthy, G. J., Silber, H. B., Rhyne, J. J., Eds.; Plenum: New York, 1982; Vol. 3. (c) *The Rare Earths in Modern Science and Technology*; McCarthy, G. J., Rhyne, J. J., Silber, H. B., Eds.; Plenum: New York, 1980; Vol. 2. (d) *The Rare Earths in Modern Science and Technology*; McCarthy, G. J., Rhyne, J. J., Eds.; Plenum: New York, 1978; Vol. 1.
(12) (a) Olken, M. M.; Verschoor, C. M.; Ellis, A. B. *Inorg. Chem.* **1986**, *25*, 80. (b) Yersin, H. *J. Chem. Phys.* **1978**, *68*, 4707.

10.1021/ic990510y CCC: $19.00
Published on Web 09/09/2000

M^{n+} counterions (e.g., Tl^+, Cs^+, Ca^{2+}, Ln^{3+}).[13,14] The spectroscopic properties of dicyanoaurate(I) and dicyanoargentate(I) compounds are largely determined by the extent of Au−Au and Ag−Ag interactions,[15−17] the existence of which leads to large red shifts in the absorption and luminescence energies relative to the corresponding monomer band energies seen in dilute solutions.

Energy transfer from dicyanoaurates(I) and dicyanoargentates(I), as donors, to lanthanide ion acceptors such as Eu(III)[18] and Dy(III)[19] has been studied in our group. More recently, the application of high pressure at low temperature has been reported to "tune" the energy transfer process in $Eu[Au(CN)_2]_3$.[20] The tunability of energy transfer to lanthanide ions is an important aspect for the design of new solid-state systems for technological purposes. Therefore, it is desirable to come up with strategies for the synthesis of new materials in which energy transfer is tuned to enhance the sensitized luminescence of the lanthanide ions. The terbium (III) ion is a good candidate as the acceptor in new materials with tunable energy transfer because one of the distinctive features of Tb(III) is the presence of absorption peaks over a very wide range of energy in the UV and visible regions (26×10^3 to 42×10^3 cm^{-1}; 20×10^3 to 21×10^3 cm^{-1}). Sensitization of the $^5D_4 \rightarrow {}^7F_J$ emission of Tb(III) can occur via energy transfer from strongly absorbing donors that exhibit near-UV or blue-visible luminescence, due to the spectral overlap with the Tb(III) absorption.[21] Dicyanoargentates(I) and dicyanoaurates(I) are good candidates as donors for Tb(III) because their luminescence energies occur over a wide range in the UV and visible regions. For example, our group has recently reported that single crystals of KCl doped with $[Ag(CN)_2^-]$ exhibit tunable luminescence over the 16×10^3 to 35×10^3 cm^{-1} range due to the formation of different $*[Ag(CN)_2^-]_n$ luminescent excimers and exciplexes.[17]

In the present investigation we report a temperature-dependent photoluminescence study to characterize energy transfer in pure crystals of $Tb[Ag(CN)_2]_3$ and $Tb[Au(CN)_2]_3$. The factors that affect the energy transfer efficiency from $[Ag(CN)_2^-]$ and $[Au(CN)_2^-]$ to Tb(III) in these systems are discussed.

Table 1. Emission Bands of the Dicyanoargentates(I), Dicyanoaurates(I), and Terbium (III)

$[Ag(CN)_2^-]$ bands[a]		$[Au(CN)_2^-]$ bands[c]		Tb(III) bands[e]	
λ_{max}^{em}, nm	assign.[b]	λ_{max}^{em}, nm	assign.[d]	λ_{max}^{em}, nm	assign.
285−300	A	300−315	I	491	$^5D_4 \rightarrow {}^7F_6$
315−330	B1	320−355	II	543	$^5D_4 \rightarrow {}^7F_5$
340−360	B2	370−395	III	584	$^5D_4 \rightarrow {}^7F_4$
390−430	C	420−450	IV	620	$^5D_4 \rightarrow {}^7F_3$
490−530	D	480−510	V	647	$^5D_4 \rightarrow {}^7F_2$
		600−640	VI	666	$^5D_4 \rightarrow {}^7F_1$
				677	$^5D_4 \rightarrow {}^7F_0$

[a] Based on ref 17. [b] Assigned to $*[Ag(CN)_2^-]_n$ ($n \geq 2$) with different "*n*" and/or different geometry. Designations follow ref 17. [c] Based on ref 15b. [d] Assigned to $*[Au(CN)_2^-]_n$ ($n \geq 2$) with different "*n*" and/or different geometry. Designations follow ref 15a. [e] Based on this work.

Experimental Section

Crystals of $M[Ag(CN)_2]_3$ (M = Tb; Gd) were prepared by slow evaporation at ambient temperature of solutions prepared by the addition of stoichiometric amounts of $M(NO_3)_3$ to aqueous solutions of $K[Ag(CN)_2]$. Crystals of $M[Au(CN)_2]_3$ (M = Tb; Y) were prepared in a similar manner from MCl_3 and $K[Au(CN)_2]$ solutions. Photoluminescence spectra were recorded with a Model QuantaMaster-1046 fluorescence spectrophotometer from Photon Technology International, PTI. The instrument is equipped with two excitation monochromators and a 75 W xenon lamp. The spectra were recorded for crystalline samples as a function of temperature between 10 K and room temperature. Liquid helium was used as the coolant in a model LT-3-110 Heli-Tran cryogenic liquid transfer system, equipped with a temperature controller, from Air Products. The excitation spectra were corrected for spectral variations in the lamp intensity by dividing the raw data by the excitation spectrum of the quantum counter rhodamine B (λ_{em} = 635 nm). Lifetime measurements were performed using a Nanolase diode-pumped solid-state laser. The laser is frequency doubled twice to give an output of 0.43 ns pulses at 266 nm with a repetition rate of 8.1 kHz. The detection system was composed of a McPherson model 2051 monochromator with a Hamamatsu R1463 photomultiplier and a Princeton Applied Research model 115 wide-band preamplifier. The data were collected using a LeCroy 9310 400 MHz digital oscilloscope. The decays were averaged over 500 sweeps on the oscilloscope and analyzed using MATLAB version 5.

Results and Discussion

1. Electronic Structures of the Cations and Anions. The energy levels of dicyanoaurate(I) and dicyanoargentate(I) species are shown in Table 1, based on the emission energies of the $[Au(CN)_2^-]_n$ and $[Ag(CN)_2^-]_n$ clusters reported elsewhere.[15,17] The luminescence bands of Tb(III) obtained in this work are also included in Table 1. The lowest-energy excited states of the Gd(III) and Y(III) cations used are $\sim 32 \times 10^3$ cm^{-1} ($\sim$310 nm) and 43×10^3 cm^{-1} ($\sim$230 nm), respectively, based on published values of the atomic energy levels for these cations.[22]

The luminescence bands of the dicyanoaurate(I) and dicyanoargentate(I) ions have been characterized as due to the formation of the metal−metal bonded excimers and exciplexes $*[M(CN)_2^-]_n$ (M = Au, Ag) with different numbers of neighboring ions (*n*) and/or geometry.[15b,17] The luminescence bands characteristic of these excimers and exciplexes are distinguished by their broadness even at cryogenic temperatures, their large Stokes shifts, and red shifts from the corresponding monomer bands. The broadness and large Stokes shifts are due to the largely distorted excimer and exciplex excited states. The

(13) (a) Omary, M. A.; Webb, T. R.; Assefa, Z.; Shankle, G. E.; Patterson, H. H. *Inorg. Chem.* **1998**, *37*, 1380. (b) Range, K. J.; Kühnel, S.; Zabel, M. *Acta Crystallogr.* **1989**, *C45*, 1419. (c) Zabel, M.; Kühnel, S.; Range, K. J. *Acta Crystallogr.* **1989**, *C45*, 1619. (d) Hoard, J. L. *Z. Kristallogr.* **1933**, *84*, 231. Staritzky, E. *Anal. Chem.* **1956**, *28*, 419. (e) Range, K. J.; Zabel, M.; Meyer, H.; Fischer, H. *Z. Naturforsch.* **1985**, *40B*, 618. (f) Hoskins, B. F.; Robson, R.; Scarlett, N. V. Y. *J. Chem. Soc., Chem. Commun.* **1994**, 2025.
(14) (a) Rosenzweig, A.; Cramer, D. T. *Acta Crystallogr.* **1959**, *12*, 709. (b) Blom, N.; Ludi, A.; Bürgi, H.-B.; Tichy, K. *Acta Crystallogr.* **1984**, *C40*, 1770.
(15) (a) Rawashdeh-Omary, M. A.; Omary, M. A.; Patterson, H. H. Oligomerization of $Au(CN)_2^-$ and $Ag(CN)_2^-$ Ions in Solution via Ground-State Aurophilic and Argentophilic Bonding. *J. Am. Chem. Soc.*, in press. (b) Rawashdeh-Omary, M. A. Ph.D. Thesis, Graduate School, University of Maine, 1999. (c) Nagle, J. K.; LaCasce, J. H., Jr.; Dolan, P. J., Jr.; Corson, M. R.; Assefa, Z.; Patterson, H. H. *Mol. Cryst. Liq. Cryst.* **1990**, *181*, 359. (d) Patterson, H. H.; Roper, G.; Biscoe, J.; Ludi, A.; Blom, N. *J. Lumin.* **1984**, *31/32*, 555. (e) Markert, J. T.; Blom, N.; Roper, G.; Perregaux, A. D.; Nagasundaram, N.; Corson, M. R.; Ludi, A.; Nagle, J. K.; Patterson, H. H. *Chem. Phys. Lett.* **1985**, *118*, 258. (f) LaCasce, J. H., Jr.; Turner, W. A.; Corson, M. R.; Dolan, P. J., Jr.; Nagle, J. K. *Chem. Phys.* **1987**, *118*, 289.
(16) Omary, M. A.; Patterson, H. H. *Inorg. Chem.* **1998**, *37*, 1060.
(17) Omary, M. A.; Patterson, H. H. *J. Am. Chem. Soc.* **1998**, *120*, 7696.
(18) Assefa, Z.; Shankle, G.; Patterson, H. H.; Reynolds, R. *Inorg. Chem.* **1994**, *33*, 2187.
(19) Assefa, Z.; Patterson, H. H. *Inorg. Chem.* **1994**, *33*, 6195.
(20) Yersin, H.; Trümbach, D.; Strasser, J.; Patterson, H. H.; Assefa, Z. *Inorg. Chem.* **1998**, *37*, 3209.
(21) Richardson, F. S. *Chem. Rev.* **1982**, *82*, 541.
(22) (a) Martin, W. C.; Zalubas, R.; Hagan, L. *Atomic Energy Levels—The Rare Earth Elements*; Nat. Bur. Stand.: Washington, 1978. (b) Chang, N. C. *J. Appl. Phys.* **1963**, *34*, 3500. (c) Wickersheim, K. A.; Lefever, R. A. *J. Opt. Soc. Am.* **1961**, *51*, 1147.

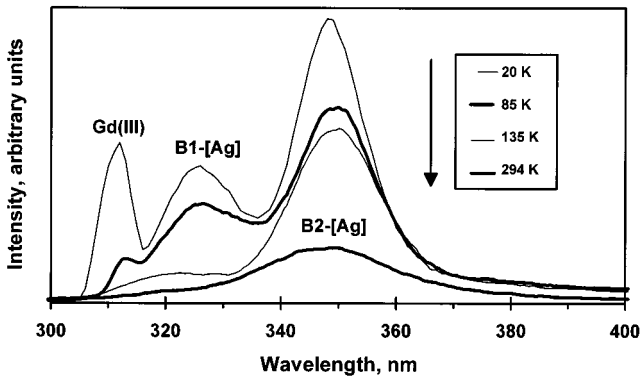

Figure 1. Emission spectra of $Gd[Ag(CN)_2]_3$ as a function of temperature using 260 nm excitation.

low energies are due to the oligomerization of $[M(CN)_2^-]$ ions as a result of excited-state M−M bonding, which leads to a reduction in the value of the HOMO−LUMO gap from the value for the corresponding monomer. The assignment of the luminescence bands of dicyanoaurate(I) and dicyanoargentate(I) ions in Table 1 is based on many spectroscopic studies of these ions in a variety of pure crystals, doped crystals, and solutions.[13−19] On the other hand, the narrow luminescence bands of the rare-earth ion Tb(III) are due to the $^5D_4 \rightarrow {}^7F_J$ ($J = 0-6$) transitions.[1]

2. Energy Transfer between $[Ag(CN)_2^-]$ and Tb(III). The luminescence properties of the $[Ag(CN)_2^-]$ donor ions are represented by $Gd[Ag(CN)_2]_3$. The excitation spectra of a single crystal of $Gd[Ag(CN)_2]_3$ show broad excitation bands in the 250−330 nm range. Figure 1 shows the emission spectra as a function of temperature using 260 nm excitation. Three emission bands are evident in Figure 1 at ca. 310, 325, and 350 nm, respectively. The full-width at half-maximum (fwhm) is ∼700 cm^{-1} for the 310 nm band compared with a fwhm value of ∼1300 cm^{-1} for the 350 nm band. The bandwidth of the 310 nm band is inconsistent with the emission bands of silver dicyanide species, which are broad due to excimer/exciplex formation.[17] Meanwhile, the energy level diagram of gadolinium(III) indicates that the lowest excited state has an energy of $\sim 32.3 \times 10^3$ cm^{-1}, which corresponds to ∼310 nm. Therefore, we assign the 310 nm emission seen in Figure 1 to the $^6P_{7/2} \rightarrow {}^8S_{7/2}$ transition in Gd(III). This assignment is consistent with the literature.[23] The 325 and 350 nm emissions are due to bands B1 and B2, respectively, of silver dicyanide species (Table 1). These bands have been assigned to two different geometrical isomers of the trimer exciplex $*[Ag(CN)_2^-]_3$.[17] The other $[Ag(CN)_2^-]$ luminescence bands listed in Table 1 were observed in $Gd[Ag(CN)_2]_3$ by controlling the excitation wavelength. However, bands B1 and B2 were the strongest.

Figure 1 shows that the 310 nm emission of Gd(III) decreases in intensity as the temperature increases. In fact, this peak disappears completely at $T > 100$ K. Figure 1 shows that band B1 becomes a less-defined shoulder as the temperature increases, which makes band B2 the prominent $[Ag(CN)_2^-]$ emission at high temperatures. The decrease of the overall luminescence intensity of $Gd[Ag(CN)_2]_3$ as the temperature increases, as shown in Figure 1, is due to the nonradiative deexcitation processes to the ground state. An increase in temperature also leads to phonon-assisted relaxation processes between the energy levels of the luminescent species. This leads to a decrease in the relative intensity of the Gd(III) emission with respect to the lower-energy $[Ag(CN)_2^-]$ bands. The change of the relative intensity of the B1 and B2 $[Ag(CN)_2^-]$ bands as a function of temperature is due to energy transfer processes between the $[Ag(CN)_2^-]_n$ clusters characteristic of these bands.[24]

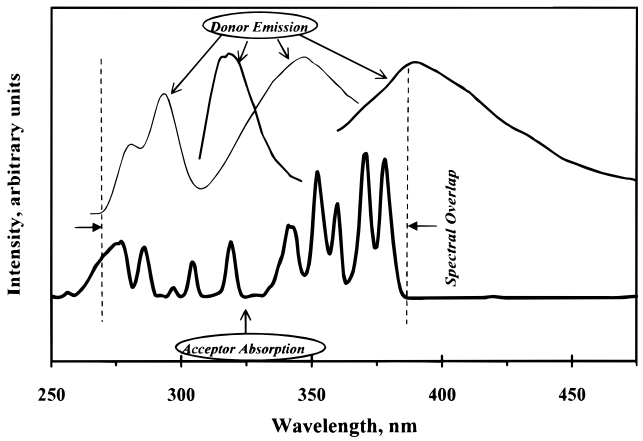

Figure 2. Spectral overlap between the $[Ag(CN)_2^-]$ donor emission in $Tb[Ag(CN)_2]_3$ at 20 K and the Tb(III) excitation in $TbCl_3$. The excitation wavelengths used for the donor emission bands shown are 245, 290, and 337 nm, respectively (left to right). The donor−acceptor spectral overlap is shown in the region between the vertical dashed lines.

The $Tb[Ag(CN)_2]_3$ compound displays a strong sensitized luminescence for Tb(III) at all temperatures studied (10−290 K). All emission lines for the $^5D_4 \rightarrow {}^7F_J$ ($J = 0-6$) transition of Tb(III) have been observed. The data shown in Table 1 for the Tb(III) emission bands are taken from the emission spectra of $Tb[Ag(CN)_2]_3$ in the Tb(III) emission region at 10 K and using 300 nm excitation. The energies and relative intensities of the Tb(III) luminescence lines obtained are consistent with the literature data.[25]

The efficiency of energy transfer is linearly dependent on the magnitude of the spectral overlap between the donor emission and the acceptor absorption. It has been established that the energy transfer rate, P_{D-A}, is governed by the expression[26−29]

$$P_{D-A} = F(R) \int I_D(\bar{\nu})\, \epsilon_A(\bar{\nu})\, d\bar{\nu} \qquad (1)$$

where the integral represents the spectral overlap between the donor emission, $I_D(\bar{\nu})$, and the acceptor absorption, $\epsilon_A(\bar{\nu})$. The factor $F(R)$ is dependent on the intermolecular distance between the donor and acceptor centers and is governed by the relevant energy transfer mechanism such as the Förster multipole mechanism[30] or the Dexter exchange mechanism.[31] Figure 2 illustrates the large spectral overlap between the $[Ag(CN)_2^-]$ donor emission and the Tb(III) acceptor absorption. The different $[Ag(CN)_2^-]$ emission bands were obtained using different

(23) (a) Pearson, A. D.; Peterson, G. E. *Appl. Phys. Lett.* **1964**, *5*, 222. (b) Reisfeld, R.; Greenberg, E.; Velapoldi, R.; Barnett, B. *J. Chem. Phys.* **1972**, *56*, 1698.

(24) Rawashdeh-Omary, M. A.; Omary, M. A.; Shankle, G. E.; Patterson, H. H. *J. Phys. Chem. B* **2000**, *104*, 6143.

(25) Bünzli, J.-C. G.; Choppin, G. R. *Lanthanide Probes in Life, Chemical and Earth Sciences*; Elsevier: Amsterdam, 1989.

(26) Reisfeld, R. *Struct. Bonding (Berlin)* **1976**, *30*, 65.

(27) Wayne, R. P. *Principles and Applications of Photochemistry*; Oxford University Press: Oxford, 1988; Chapter 5.

(28) Cowan, D. O.; Drisko, R. L. *Elements of Organic Photochemistry*; Plenum Press: New York, 1976; Chapter 6.

(29) Adamson, A. W.; Fleischauer, P. D. *Concepts of Inorganic Photochemistry*; Wiley-Interscience: New York, 1975; pp 72−77.

(30) Förster, T. *Fluoreszenz Organischer Verbindungen*; Vandenhoeck und Ruprecht: Göttingen, Germany, 1951.

(31) Dexter, D. L. *J. Chem. Phys.* **1953**, *21*, 836.

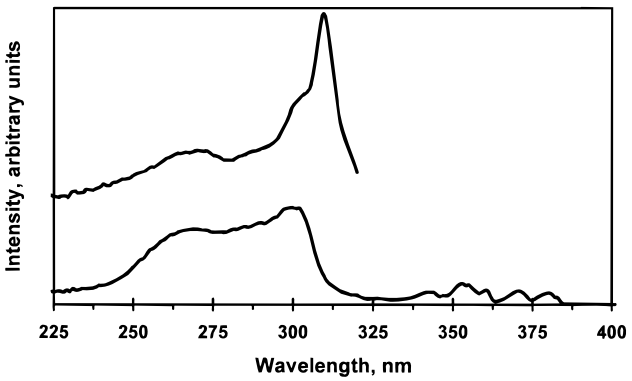

Figure 3. Comparison of the corrected excitation spectra of the Tb(III) emission (λ_{em} = 543 nm) in $Tb[Ag(CN)_2]_3$ (bottom) and the $[Ag(CN)_2^-]$ emission (λ_{em} = 350 nm) in $Gd[Ag(CN)_2]_3$ (top) at 10 K.

excitation wavelengths (see Table 1 for the assignment). A strikingly large spectral overlap of the donor emission with the acceptor absorption is quite evident in Figure 2. This spectral overlap occurs over a rather broad spectral range due to the several emission centers of the $[Ag(CN)_2^-]$ donor that coincide with the absorption bands of the acceptor. These emission centers are attributed to different excited-state oligomers (exciplexes) of $*[Ag(CN)_2^-]_n$ species.[17] The spectra shown in Figure 2 indicate a high value for the integral representing the spectral overlap between the donor emission, $I_D(\bar{\nu})$, and the acceptor absorption, $\epsilon_A(\bar{\nu})$, in eq 1.

In Figure 3, the excitation peak of $Tb[Ag(CN)_2]_3$ monitoring the Tb(III) emission is shown to have a shape and energy similar to those of the excitation peak of $Gd[Ag(CN)_2]_3$ monitoring the $[Ag(CN)_2^-]$ emission. It is well-known that the increased intensity of the excitation profile of the rare earth ion luminescence in the region of the excitation peak of the donor is indicative of energy transfer. This method has been used to confirm the presence of energy transfer in many biochemical[21,32−37] and inorganic systems.[18,38−40] The enhancement of the excitation bands of the Tb(III) sensitized luminescence in $Tb[Ag(CN)_2]_3$ can be realized by comparing the excitation spectra of $Tb[Ag(CN)_2]_3$ in Figure 3 with the excitation spectrum of solid $TbCl_3$ (Figure 2). It is clear that the Tb(III) emission is enhanced in the region of the excitation spectrum that corresponds to the $[Ag(CN)_2^-]$ donor.

We have studied the temperature dependence of the $Tb[Ag(CN)_2]_3$ luminescence using different excitation wavelengths. Figure 4 shows the emission spectra versus temperature of $Tb[Ag(CN)_2]_3$ using 310 nm excitation. The enhancement of the acceptor emission concomitant with the quenching of the donor emission has been used as evidence for the presence of energy transfer in many previous studies.[18−19,21,41] Efficient energy transfer from $[Ag(CN)_2^-]$ to Tb(III) in $Tb[Ag(CN)_2]_3$ is

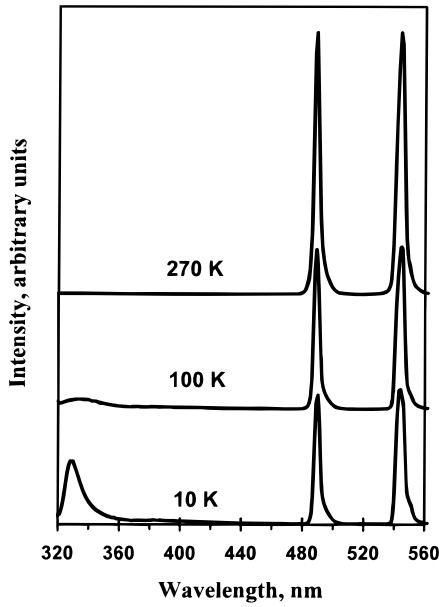

Figure 4. Emission spectra of $Tb[Ag(CN)_2]_3$ as a function of temperature using 310 nm excitation.

Table 2. Emission Intensity Ratio of the Acceptor/Donor in $Tb[Ag(CN)_2]_3$ as a Function of Temperature[a]

T, K	10	37	56	83	100	165	202	240	268	294
$I[Tb^{3+}]/I([Ag])$	2.13	3.44	6.48	12.0	17.3	41.6	68.8	100	175	244

[a] Based on the peak heights of the Tb(III) emission band at ~491 nm and the major $[Ag(CN)_2^-]$ emission band at ~330 nm.

expected, therefore, to result in a strong luminescence in the Tb(III) region concomitant with a quenching of the $[Ag(CN)_2^-]$ luminescence. The emission spectra of $Tb[Ag(CN)_2]_3$ at 10 K using different excitation wavelengths show that, overall, the $[Ag(CN)_2^-]$ emission is much weaker than the Tb(III) emission. Dicyanoargentate(I) species are strong emitters at cryogenic temperatures.[16,17] The quenching of this otherwise strong luminescence is an illustration of efficient energy transfer from $[Ag(CN)_2^-]$ to Tb(III) in $Tb[Ag(CN)_2]_3$.

Figure 4 shows that as the temperature is increased toward room temperature, the Tb(III) acceptor emission is enhanced gradually while the $[Ag(CN)_2^-]$ emission becomes totally quenched. The temperature dependence for the $Tb[Ag(CN)_2]_3$ emission shown in Figure 4 is an indication that energy transfer is enhanced with a temperature increase. Table 2 summarizes the emission intensity data versus temperature using 310 nm excitation. It is noted that the intensity ratio of the acceptor/donor emission increases gradually as a function of temperature. Similar trends have been obtained upon excitation with other wavelengths in the range of the $[Ag(CN)_2^-]$ absorption. The observation of temperature-activated enhancement in the Tb(III) emission up to room temperature indicates that the energy transfer process competes favorably with the nonradiative decay of the excitation energy of the donor. That is, the energy transfer rate is greater than the rate of the thermal nonradiative decay of the donor excitation to its ground state. Assuming a simple two-level system as the phenomenological model for energy transfer from $[Ag(CN)_2^-]$ donors to the Tb(III) acceptor, it is possible to evaluate the energy transfer rates in $Tb[Ag(CN)_2]_3$ from the relative intensity of the acceptor emission.[1] A quantitative analysis of the data has revealed an exponential increase of the energy transfer rate as temperature increases. If the Tb(III) emission intensity is determined only by energy transfer, the energy transfer rate can be obtained by an Arrhenius equation

(32) Monasterio, O.; Acoria, M.; Díaz, M. A.; Lagos, R. *Arch. Biochem. Biophys.* **1993**, *300*, 582.
(33) Sherry, A. D.; Au-Young, S.; Cottam, G. L. *Arch. Biochem. Biophys.* **1978**, *189*, 277.
(34) Rübsamen, H.; Hess, G. P.; Eldefrawi, A. T.; Eldefrawi, M. E. *Biochem. Biophys. Res. Commun.* **1976**, *68*, 56.
(35) Luk, C. K. *Biochemistry* **1971**, *10*, 2838.
(36) Richardson, C. E.; Behnke, W. D. *Biochim. Biophys. Acta* **1978**, *534*, 267.
(37) Ringer, D. P.; Etheredge, J. L.; Dalrymple, B. L.; Niedbalski, J. S. *Biochem. Biophys. Res. Commun.* **1990**, *168*, 267.
(38) Blasse, G.; Bokkers, G.; Dirksen, G.; Brixner, L. *J. Solid State Chem.* **1983**, *60*, 803.
(39) Chang, N. C. *J. Appl. Phys.* **1963**, *34*, 3500.
(40) de Hair, J. T. W. *J. Lumin.* **1979**, *18/19*, 797.
(41) Horrocks, W. DeW., Jr.; Albin, M. *Prog. Inorg. Chem.* **1984**, *31*, 1.

Table 3. Lifetimes for the Tb(III) Emission at 491 nm as a Function of Temperature for $Tb[Ag(CN)_2]_3$ and $Tb[Au(CN)_2]_3$

	temp (K)	lifetime (μs)
$Tb[Ag(CN)_2]_3$	80	320(20)
	130	350(10)
	200	380(10)
$Tb[Au(CN)_2]_3$	80	500(40)
	170	370(20)

of the form

$$k_{ET}(T) = (k_{ET})_{T\to\infty} \exp(-E_a/RT) \qquad (2)$$

where k_{ET} is the energy transfer rate, E_a is the energy of activation for the transfer process, and R is the gas constant. The value of k_{ET} at a given temperature is proportional to the relative emission intensity of Tb(III) at that temperature ($I_{Tb}(T)$). A plot of ln $I_{Tb}(T)$ vs $1/T$ should give a straight line if energy transfer is the only mechanism responsible for the Tb(III) intensity. An Arrhenius plot monitoring the 490 nm line has given a reasonably good linear fit ($R^2 = 0.989$). The equation of the straight line obtained ($\ln I_{490nm} = -77.249/T + 14.213$) leads to an activation energy of 53.7 cm^{-1} (± 2.5 cm^{-1}). Similar calculations of the activation energy to rare-earth ions have been reported for antiferromagnets of Mn^{2+},[42] dicyanoaurates(I),[43] and tetracyanoplatinates(II).[44]

The temperature dependence of energy transfer in $Tb[Ag(CN)_2]_3$ can be explained in terms of an exciton model. The equilibrium geometry of the excited state of the $*[Ag(CN)_2^-]_n$ donor species is markedly different from the corresponding ground-state equilibrium geometry. This is true because of exciplex formation in dicyanoargentate(I) species, which leads to large reductions in the equilibrium Ag−Ag distances in the excited states relative to the ground states. As a result, the excitation energy of the excited donor undergoes significant lattice relaxation before energy transfer takes place. This leads to the localization of the resulting electronic states to a few linear $[Ag(CN)_2^-]$ ions in a given layer, as opposed to the delocalization of the exciton over all the $[Ag(CN)_2^-]$ ions in the layer. This process is reminiscent of the so-called "self-trapping" process that has been well established in the tetracyanoplatinates(II).[44−46] Due to the good match between the donor emission and the acceptor absorption (Figure 2), the value of the activation barrier for the energy transfer in $Tb[Ag(CN)_2]_3$ is expected to be small and energy transfer should proceed even at low temperatures, as observed experimentally. This explains the small value of 53.7 cm^{-1} (± 2.5 cm^{-1}) for the activation energy of the transfer process. An increase in temperature helps overcome the activation barrier and, consequently, increases the efficiency of energy transfer in $Tb[Ag(CN)_2]_3$.

We have obtained lifetimes for the Tb(III) emission at 491 nm at several temperatures (Table 3). The acceptor lifetime increases from 320(20) to 380(10) μs upon heating the sample from 80 to 200 K. This result is in agreement with the steady-state luminescence data, which show an increase in the relative intensity of the Tb(III) emissions with increasing temperature. As the donor emission was almost completely quenched at temperatures $\geq$80 K, it was not detectable for the purposes of lifetime measurements.

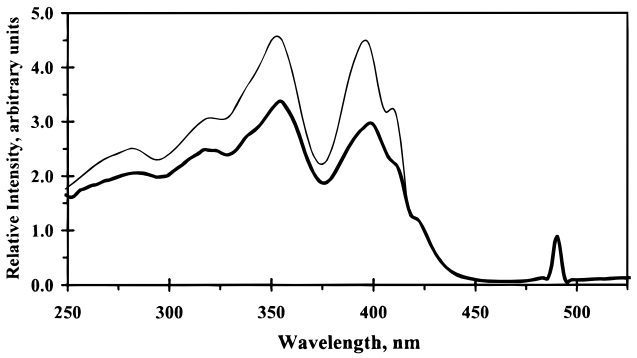

Figure 5. Comparison between the corrected excitation spectra of $Tb[AuCN)_2]_3$ at 10 K monitoring the Tb(III) emission ($\lambda_{max} = 588$ nm, bottom) and the $[AuCN)_2^-]$ emission ($\lambda_{max} = 440$ nm, top).

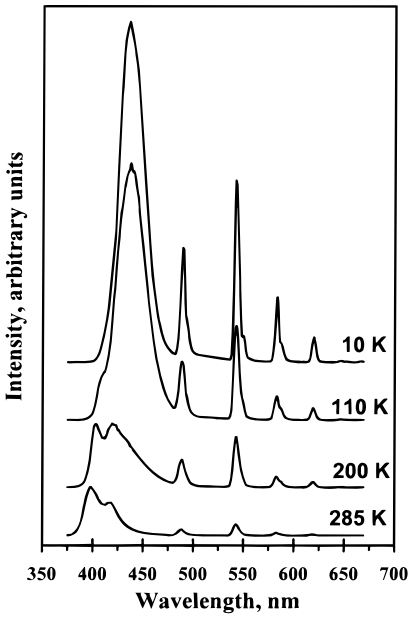

Figure 6. Emission spectra of $Tb[AuCN)_2]_3$ as a function of temperature using 350 nm excitation.

3. Energy Transfer between $[Au(CN)_2^-]$ and Tb(III). The luminescence properties of the $[Au(CN)_2^-]$ donor ions are represented by $Y[Au(CN)_2]_3$. Three emissions due to $[Au(CN)_2^-]$ have been observed in $Y[Au(CN)_2]_3$ at 393, 450, and 490 nm. Several excitation peaks have been observed between 260 and 450 nm. Excitation with different wavelengths has resulted in similar emission spectra. Energy transfer from $[Au(CN)_2^-]$ as the donor to Tb(III) as the acceptor has been studied. The occurrence of Tb(III) luminescence in $Tb[Au(CN)_2]_3$ via energy transfer mechanism from the $[Au(CN)_2^-]$ donor is illustrated in Figure 5. There is a strong resemblance between the excitation spectra that monitor the Tb(III) luminescence and those that monitor the $[Au(CN)_2^-]$ luminescence, according to Figure 5. This provides evidence for the presence of donor−acceptor energy transfer, as discussed earlier in the $Tb[Ag(CN)_2]_3$ case.

Figure 6 shows the emission spectra of $Tb[Au(CN)_2]_3$ as a function of temperature. The broad bands near 400 and 450 nm and the weak shoulder near 500 nm are due to $[Au(CN)_2^-]$ luminescence. The sharp bands in the low-energy region in Figure 6 are due to the $^5D_4 \rightarrow {}^7F_J$ ($J = 0-6$) sensitized luminescence of Tb(III). The temperature dependence of the

(42) Kambli, U.; Güdel, H. U. *Inorg. Chem.* **1984**, *23*, 3479.
(43) Nagasundaram, N.; Roper, G.; Biscoe, J.; Chai, J. W.; Patterson, H. H.; Blom, N.; Ludi, A. *Inorg. Chem.* **1986**, *25*, 2947.
(44) (a) Yersin, H.; Gliemann, G. *Ann. N.Y. Acad. Sci.* **1978**, *313*, 539. (b) Gliemann, G.; Yersin, H. *Struct. Bonding* **1985**, *62*, 87.
(45) Rössler, U.; Yersin, H. *Phys. Rev.* **1982**, *B26*, 3187 and references therein.
(46) (a) Yersin, H.; von Ammon, W.; Stock, M.; Gliemann, G. *J. Lumin.* **1979**, *18/19*, 774. (b) Yersin, H.; Stock, M. *J. Chem. Phys.* **1982**, *76*, 2136.

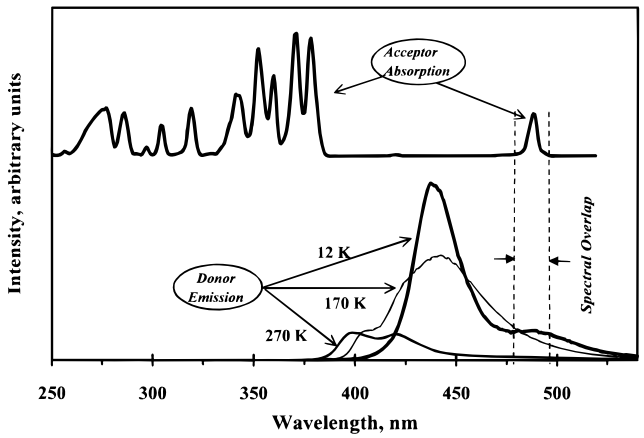

Figure 7. Spectral overlap between the $[AuCN)_2^-]$ donor emission in $Y[Au(CN)_2]_3$ at different temperatures and the Tb(III) excitation in $TbCl_3$. The donor−acceptor spectral overlap is shown in the region between the vertical dashed lines.

$[Au(CN)_2^-]$ luminescence in $Tb[Au(CN)_2]_3$ shows the same trends as in $Y[Au(CN)_2]_3$. All $[Au(CN)_2^-]$ emission bands undergo blue shifts with increasing temperature. This is a well-known trend for the dicyanoaurates(I) and other layered compounds. For example, the $K[Au(CN)_2]$ luminescence blue shifts by 1100 cm^{-1} upon increasing the temperature from 78 to 300 K.[43] The shift to lower luminescence energies of low-dimensional layered compounds upon cooling is a result of the thermal reduction of the metal−metal distances.[15−17,44,47,48] Another observation in Figure 6 is the increase of the relative intensities of the higher-energy luminescence bands of $[Au(CN)_2^-]$ as the temperature increases. For example, the highest-energy band at ~395 nm is virtually absent at 10 K but becomes the major band at 285 K. Energy transfer between $*[Au(CN)_2^-]_n$ luminescent clusters is responsible for the changes in the relative intensities of the luminescence bands characteristic of $[Au(CN)_2^-]$ in both $Y[Au(CN)_2]_3$ and $Tb[Au(CN)_2]_3$. The increase of the relative intensities of the higher-energy bands with a temperature increase is an indication of "back-transfer" from low-energy levels to high-energy levels. Back-transfer is not unusual in coordination compounds. For example, Kambli and Güdel have reported back-transfer in antiferromagnets of Mn^{2+}.[42] The back-transfer between $*[Au(CN)_2^-]_n$ species in $Y[Au(CN)_2]_3$ and $Tb[Au(CN)_2]_3$ is a phonon-assisted process due to C−N vibrations ($\nu_{C-N} \cong 2200$ cm^{-1}).

Figure 6 shows that the Tb(III) luminescence decreases in intensity upon increasing the temperature. It is also noted in Figure 6 that the $[Au(CN)_2^-]$ luminescence is strong at all temperatures. The efficiency of energy transfer in $Tb[Au(CN)_2]_3$ is assessed by studying the spectral overlap of the donor emission with the acceptor absorption (eq 1). Figure 7 illustrates the spectral overlap between the $[Au(CN)_2^-]$ donor emission and the Tb(III) acceptor excitation as a function of temperature. It is noted that the donor emission overlaps with only one acceptor absorption line, the $^5D_4 \rightarrow {}^7F_6$ band at ~490 nm. Moreover, the overlapping donor emission comes only from the shoulder near 500 nm. The donor−acceptor spectral overlap increases upon cooling because the $[Au(CN)_2^-]$ emission shifts in the direction of this low-energy shoulder. This explains why energy transfer from $[Au(CN)_2^-]$ to Tb(III) in $Tb[Au(CN)_2]_3$ is "tuned-in" by decreasing the temperature.

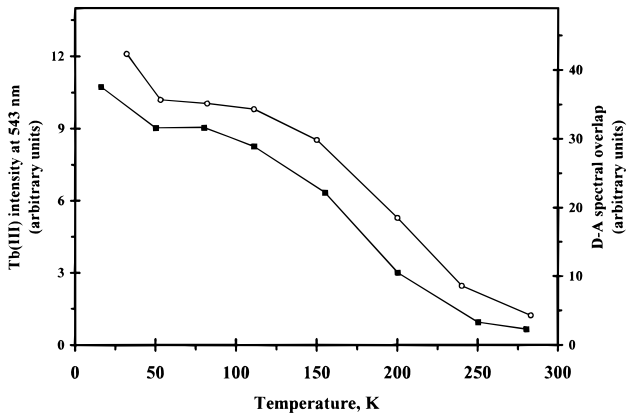

Figure 8. Comparison between the Tb(III) sensitized emission intensity in $Tb[Au(CN)_2]_3$ (top) and the value of the donor−acceptor spectral overlap (bottom) as a function of temperature.

Because the $[Au(CN)_2^-]$ emission in $Tb[Au(CN)_2]_3$ is strong and does not undergo a complete quenching at all temperatures studied, it was possible to determine the values of the spectral overlap integral with the Tb(III) absorption. A comparison between Figures 6 and 7 indicates that the profile of the $[Au(CN)_2^-]$ emission versus temperature is similar in $Tb[Au(CN)_2]_3$ to that in $Y[Au(CN)_2]_3$. Therefore, in the calculation of the donor−acceptor spectral overlap it is reasonable to use the emission spectra of $Y[Au(CN)_2]_3$ to represent the donor emission. The calculations have been carried out for the overlap of the $[Au(CN)_2^-]$ donor emission with the $^5D_4 \rightarrow {}^7F_6$ absorption band of Tb(III) (as illustrated in Figure 7). In Figure 8, the numerical values of the donor−acceptor spectral overlap are shown and compared with the sensitized emission intensity of Tb(III) versus temperature. The Tb(III) sensitized emission intensity in $Tb[Au(CN)_2]_3$ varies with temperature in a manner very similar to that of the spectral overlap, according to Figure 8. This provides a nice illustration of eq 1, which predicts that the energy transfer rate (represented herein by the Tb(III) sensitized emission intensity) is directly proportional to the donor−acceptor spectral overlap. The tunability of the nonradiative energy transfer rate in $Tb[Au(CN)_2]_3$ with temperature is, therefore, explained in terms of the donor−acceptor spectral overlap, as predicted by theory and as demonstrated in Figure 8. Only a few reported examples have demonstrated this correlation experimentally by application of high pressure,[20,46] whereas in $Tb[Au(CN)_2]_3$ here the tunability is achieved by temperature variation.

We can also demonstrate energy transfer in $Tb[Au(CN)_2]_3$ by investigating the luminescence decay characteristics of the donor and acceptor. We show both the donor and acceptor decay at 80 K in Figure 9. The acceptor decay is exponential, with a lifetime of 500(40) μs at 80 K. This lifetime decreases upon heating to 370(20) μs at 170 K (Table 3). This decrease in the Tb(III) lifetime with an increase in temperature is in agreement with the steady-state luminescence data, which show a decreased relative intensity for the Tb(III) emissions upon increasing the temperature. Figure 9 also shows that the donor decay is nonexponential at the short time domain. It is well-known that nonexponential donor decay indicates the presence of energy transfer,[49] as it has been demonstrated in the literature for a variety of donor−acceptor systems.[50]

4. Mechanism of Energy Transfer. We propose that the mechanism of energy transfer in both $Tb[Ag(CN)_2]_3$ and $Tb[Au(CN)_2]_3$ is the Dexter exchange mechanism. Such a mechanism is followed in systems that have a short donor−acceptor

(47) Yersin, H.; Riedl, U. *Inorg. Chem.* **1995**, *34*, 1642.
(48) Connick, W. B.; Henling, L. M.; Marsh, R. E.; Gray, H. B. *Inorg. Chem.* **1996**, *35*, 6261.

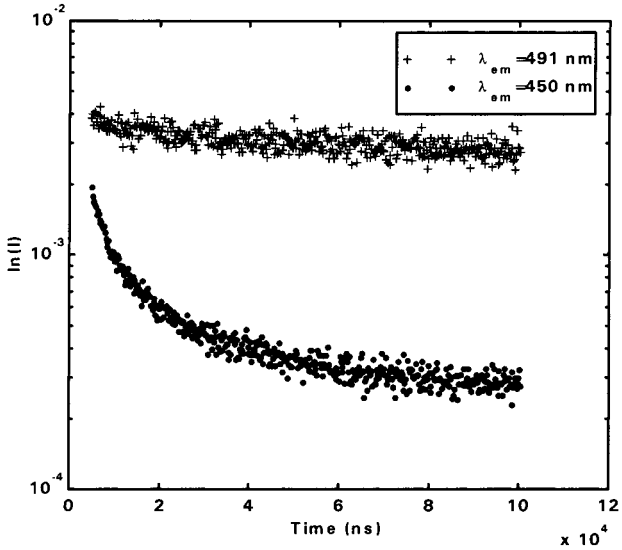

Figure 9. Log plot of the luminescence decay for the Tb(III) acceptor (top) (491 nm) and the donor (bottom) (450 nm) in $Tb[Au(CN)_2]_3$ at 80 K. Note the nonexponential character of the donor decay indicative of energy transfer.

separation. The Dexter exchange mechanism assumes the occurrence of a bimolecular encounter (collision) between the donor and the acceptor.[26−29,31,51] Therefore, such a mechanism is dominant when the donor−acceptor distance is short and when significant overlap exists between the molecular orbitals of the two species. On the other hand, the Förster resonance mechanism can occur over donor−acceptor distances as long as 50−100 Å.[30,31,51] The crystal structures of various $Ln[M(CN)_2]_3$ (M = Au, Ag) have been determined and show that Ln(III) ions such as Tb(III) are directly bonded to the cyanide ligands of $[M(CN)_2^-]$ with short Ln−N distances.[18,52] For example, a Tb−N distance of 2.45 Å is present in $Tb[Au(CN)_2]_3$.[52a] The crystal structure of $Tb[Ag(CN)_2]_3$ has not been determined yet, but the electronic factors that govern the Tb−N interactions are similar to those in the analogous gold compound. Furthermore, it has been suggested that the LUMOs of dicyanoargentate(I) and dicyanoaurate(I) species have a mixed character between the Ag (or Au) atom and the CN^- ligand (mostly cyanide character).[16,17,53−56] The electron densities of the LUMOs extend beyond the nitrogen atoms of the cyanide ligands,[55,56] thus facilitating the overlap with the 4f orbitals of the Tb(III) ions. We conclude on the basis of this discussion that the Dexter exchange mechanism is responsible for the energy transfer in $Tb[Ag(CN)_2]_3$ and $Tb[Au(CN)_2]_3$. In a recent study, Yersin et al. have suggested that energy transfer in $Eu[Au(CN)_2]_3$ also follows the Dexter mechanism.[20]

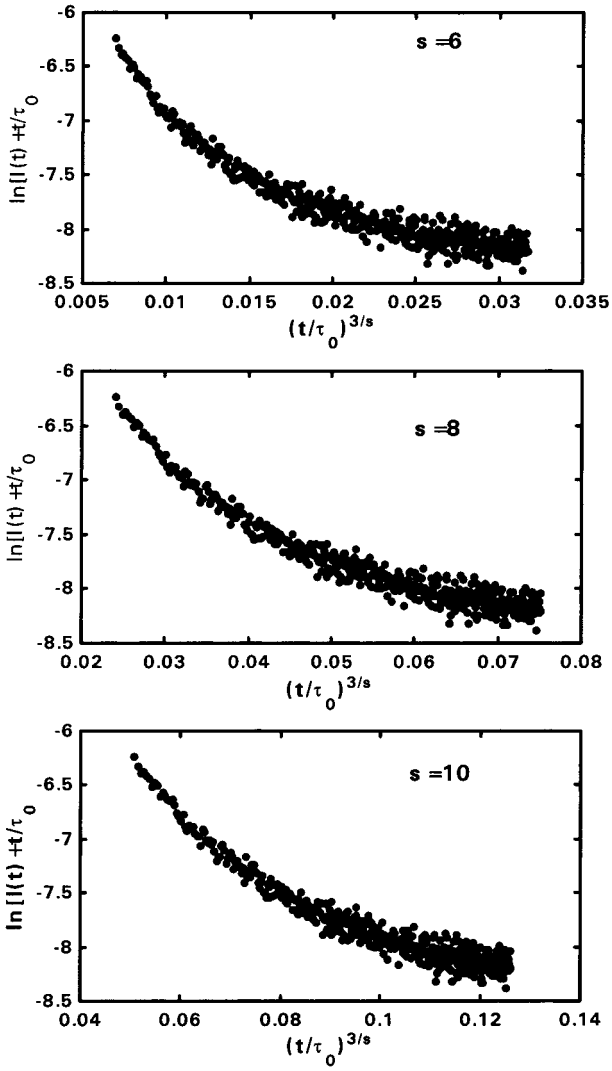

Figure 10. Plots of $\ln[I(t)] + t/\tau_0$ vs $(t/\tau_0)^{3/s}$ for $s = 6$, 8, and 10. The luminescence decay is monitored for the donor emission (450 nm) in $Tb[Au(CN)_2]_3$ at 80 K.

We have used time-resolved measurements to rule out several mechanisms of energy transfer that occur via a multipolar interaction. Energy transfer via a multipolar interaction can be described by the equation[49]

$$I(t) = I(0)\exp\left[-\frac{t}{\tau_0} - \Gamma\left(1-\frac{3}{s}\right)\frac{c}{c_0}\left(\frac{t}{\tau_0}\right)^{3/}s\right] (2) \qquad (3)$$

where τ_0 is the intrinsic lifetime of the donor, c is the acceptor concentration, c_0 is a parameter called the critical transfer concentration, and $s = 6$, 8, or 10 for dipole−dipole, dipole−quadrupole, or quadrupole−quadrupole interactions, respectively. After some manipulation,[50c] plots of $\ln[I(t)] + t/\tau_0$ vs $(t/\tau_0)^{3/s}$ should give a straight line if the transfer mechanism occurs via a multipolar interaction. None of these plots with $s = 6$, 8, and 10 has resulted in a straight line for the donor decay in $Tb[Au(CN)_2]_3$ (Figure 10), suggesting a mechanism other than multipolar interaction (in agreement with our conclusion above that the mechanism is the Dexter exchange mechanism).

Concluding Remarks

This study has identified interesting trends for energy transfer processes in pure crystals of Tb(III) with dicyanoaurates(I) and dicyanoargentates(I). The efficiency of energy transfer in these

(49) Inokuti, M.; Hirayama, F. *J. Chem. Phys.* **1965**, *43*, 1978.
(50) For recent examples, see: (a) Hayakawa, T.; Kamata, N.; Yamada, K. *J. Lumin.* **1996**, *68*, 179. (b) von Arx, M. E.; Burattini, E.; Hauser, A.; van Pieterson, L.; Pellaux, R.; Decurtins, S. *J. Phys. Chem. A* **2000**, *104*, 883. (c) Yamase, T.; Naruke, H. *J. Phys. Chem. B* **1999**, *103*, 8850.
(51) Watts, R. K. In *Optical Properties of Ions in Solids*; DiBartolo, B., Ed.; Plenum Press: New York, 1975; p 307.
(52) (a) Stier, A. M. M.S. Thesis, University of Regensburg, 1996. (b) Assefa, Z.; Staples, R. D.; Fackler, J. P., Jr.; Patterson, H. H.; Shankle, G. *Acta Crystallogr.* **1995**, *C51*, 2527.
(53) Omary, M. A.; Patterson, H. H.; Shankle, G. *Mol. Cryst. Liq. Cryst.* **1996**, *284*, 399.
(54) Assefa, Z.; DeStefano, F.; Garepapaghi, M. A.; LaCasce, J. H., Jr.; Ouellete, S.; Corson, M. R.; Nagle, J. K.; Patterson, H. H. *Inorg. Chem.* **1991**, *30*, 2868.
(55) Sano, M.; Adachi, H.; Yamatera, H. *Bull. Chem. Soc. Jpn.* **1982**, *55*, 1022.
(56) Interrante, L. V.; Messmer, R. P. *Chem. Phys. Lett.* **1974**, *26*, 225.

systems is strongly dependent on the extent of the spectral overlap between the donor emission and the acceptor absorption, and also on temperature. Our data indicate that energy transfer is present in both $Tb[Ag(CN)_2]_3$ and $Tb[Au(CN)_2]_3$, resulting in Tb(III) sensitized luminescence in both compounds. The data further indicate that energy transfer is more efficient in $Tb[Ag(CN)_2]_3$ than in $Tb[Au(CN)_2]_3$. In fact, this difference is recognized visibly by the eye as the $Tb[Ag(CN)_2]_3$ crystal displays a strong green luminescence characteristic of the Tb(III) sensitized emission, while the $Tb[Au(CN)_2]_3$ crystal displays a blue luminescence characteristic of the $[Au(CN)_2^-]$ emission. Figure 11 summarizes the difference between these two compounds in terms of an energy level model. The model depicts the energy levels of the donors and the acceptor based on the experimental data for the donor emissions and the acceptor absorption (Figures 2 and 7). The matching between the $[Ag(CN)_2^-]$ emission levels and the Tb(III) absorption levels is unmistakable (Figure 11). This excellent match occurs between many donor−acceptor level pairs, resulting in a rather efficient energy transfer in $Tb[Ag(CN)_2]_3$. On the other hand, there is a match between only one donor−acceptor level pair in $Tb[Au(CN)_2]_3$, resulting in a less efficient energy transfer.

In systems where a strong donor−acceptor spectral overlap exists at all temperatures, such as $Tb[Ag(CN)_2]_3$, increasing the temperature leads to a more efficient energy transfer. The reason is that energy transfer in the systems studied is a radiationless process that occurs by the Dexter exchange mechanism. Consequently, the efficiency of this nonradiative (thermal) process is enhanced by a temperature increase. On the other hand, in systems that exhibit weaker donor−acceptor spectral overlap, such as $Tb[Au(CN)_2]_3$, energy transfer is "tuned off" by increasing the temperature. The reason is that the donor emission that overlaps with the acceptor absorption shifts to higher energies upon a temperature increase, causing a decrease in the spectral overlap with the acceptor absorption.

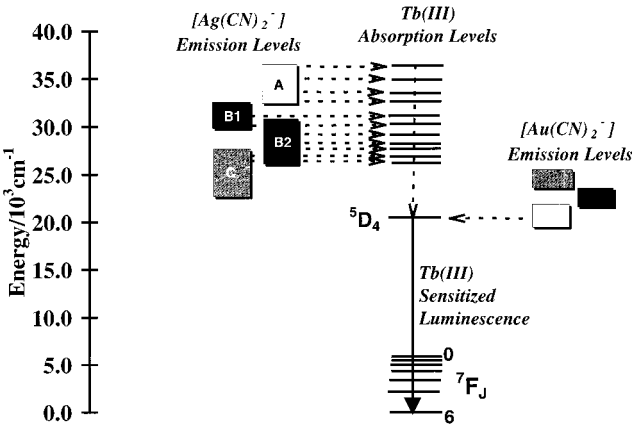

Figure 11. Energy transfer pathways from $[AgCN)_2^-]$ and $[AuCN)_2^-]$ to Tb(III). The donor and acceptor energy levels are taken from the experimental data in Figures 2 and 7. The width of a given donor emission level is based on the fwhm value, and the darkness represents the band intensity. Solid and dashed arrows represent radiative and nonradiative pathways, respectively.

Acknowledgment is made to the donors of the Petroleum Research Fund, administered by the American Chemical Society, for the support of this research.

IC990510Y